Design of double-zone aspheric diffractive intraocular lens with extended depth of focus

Yayan Bian (边亚燕), Yongji Liu (刘永基)*, and Lai Jiang (姜 来)

Institute of Modern Optics, Nankai University, Tianjin 300350, China
**Corresponding author: yjliu@nankai.edu.cn*

Received May 21, 2018; accepted July 25, 2018; posted online August 29, 2018

A double-zone aspheric diffractive intraocular lens (IOL) was designed and manufactured aiming to regain a continuous range of clear vision for pseudophakic presbyopia. After obtaining the IOL structure parameters through optimization based on an aphakic model eye, its imaging performances were analyzed in the model eye. The modulation transfer function at 50 cycles/mm remained above 0.29 within ±5° field of view for object distance ranging from 6 to 0.66 m. In addition, the imaging qualities are robust for pupil changes, polychromatic light, and different corneal asphericities. The manufactured IOL exhibits the ability to extend depth of focus.

OCIS codes: 330.4460, 220.2740, 330.7323, 050.1965.
doi: 10.3788/COL201816.093301.

The accommodation amplitude of the human eye decreases almost linearly with age at a rate of about 0.2 diopter (D) per year[1]. It usually decreases to less than 1 D after 50 years old, resulting in an inability to focus near objects accurately. This dysfunction is called presbyopia, which makes it impossible for human eyes to obtain clear vision over a continuous object range from distance to near. In addition, the crystalline lens may become cloudy, resulting in cataract, which is the most common cause of blindness and visual impairment[2]. The implantation of an intraocular lens (IOL) to replace the crystalline lens is a mature method in clinical practice[3]. Using the specially designed IOLs[4] to regain continuous clear vision is the ultimate goal for pseudophakic presbyopia. Many attempts have been made in this research area.

Bifocal IOLs[5] attempt to provide distance and near vision. Multifocal IOLs[6–8] attempt to allow distance, near, and intermediate vision to be corrected simultaneously, yet they fails to provide continuous clear vision. Accommodative IOLs[9–12] overcome the defects of bifocal and multifocal IOLs, making the axial movements possible by the special design or the use of special materials, but the provided adjustment is currently very limited. Therefore, the extended depth of focus (EDOF) IOL is proposed, aiming to provide clear images in a continuous vision range from distance to near. The TECNIS Symfony® IOL using diffractive technology by Johnson & Johnson Vision Care, Inc. (JJVCI) now is commercially available, claiming that a 1.5 D defocus vision range can be provided, but its technical details have not yet been announced[13].

There are also some other EDOF IOLs in research for vision correction. Light sword lenses[14,15] are proposed as an IOL, exhibiting great potential to extend the depth of focus (DOF) for the human eye, though it causes a loss of distance visual acuity. A multifocal IOL designed by Fernández[16] demonstrates theoretically that the modulation transfer function (MTF) at 50 cycles/mm (c/mm) remained above 0.47 for object distance ranging from 5 m to 0.4 m. The aspheric diffractive IOL proposed by Jiang *et al.*[17] provides continuous vision for object distance ranging from 0.4 to 8 m. One limit of this design is a relatively small optical zone, which is 4.5 mm in diameter.

For commercial application, an optical zone of 6 mm is generally required. Furthermore, the human eyes work in white light conditions and under different illumination, which causes pupil diameter changes. These factors require the IOLs to provide robust imaging performance under polychromatic light with different pupil sizes. Besides, the IOLs are also required to provide robust imaging for different corneal asphericites due to the individual difference of corneal asphericity.

This Letter is aimed to design an IOL, which can not only provide a 1.5 D DOF, but also meet the above requirements. A double-zone aspheric diffractive IOL with EDOF was obtained by the optimization in Zemax. Subsequently, this IOL was manufactured. The experimental result shows that the manufactured IOL exhibits the ability to extend the DOF.

An aphakic model eye with an axial length of 23.471 mm was used for IOL optimization. The parameters of the aphakic model eye are shown in Table 1.

The material of the IOL is chosen to be the polymethyl methacrylate (PMMA) material with a refractive index of 1.494 and an Abbe number of 57.5. The IOL with a 6 mm optical zone was placed 3.5 mm behind the cornea's posterior surface. The wavelength was set to be 550 nm because the human eye is the most sensitive to this wavelength. The field of view (FOV) is set to be 0°. The optical design Zemax software (Zemax OpticStudio 16.5 SP5, Premium Edition) was used to build the model eye and perform the optimization and analyses of the IOL.

The IOL surfaces are described by aspheric surfaces with two concentric optical zones. The two concentric zones are divided by two radial coordinates A_1 and A_2

Table 1. Structural Parameters of the Model Eye

Component	Radius (mm)	Conic	Thickness (mm)	Refractive Index
Anterior cornea	7.8	−0.18	0.5	1.376
Posterior cornea	6.6	−0.07	3.5	1.336
Pupil	Infinity	0	0	1.336
Anterior IOL	–	–	–	1.494
Posterior IOL	–	–	–	1.336
Retina	−12.5	–	–	–

$(0 < A_1 < A_2)$ with independent radius, conic, and aspherical coefficients. The geometry of the inner zone $(r \le A_1)$ of the IOL surfaces is described by

$$Z_1 = \frac{c_1 r^2}{1+\sqrt{1-(1+k_1)c_1^2 r^2}} + \sum_{i=1}^{N} \alpha_{1i} r^{2i}, \quad (r \le A_1). \quad (1)$$

A similar expression of the outer zone $(A_1 < r < A_2)$ with different coefficients and an offset value is given by

$$Z_2 = Z_0 + \frac{c_2 r^2}{1+\sqrt{1-(1+k_2)c_2^2 r^2}} + \sum_{i=1}^{N} \alpha_{2i} r^{2i}, \quad (A_1 < r < A_2), \quad (2)$$

where Z_0 is chosen to make the surface continuous across the boundary between the inner and outer zones or $Z_0 = Z_1(A_1) - Z_2(A_1)$. In the present study, the inner zone is 3.5 mm ($A_1 = 1.75$ mm), and the outer zone is 6 mm ($A_2 = 3$ mm).

The design steps of the IOL are as follows.

(1) A 22 D monofocal IOL with the radii of curvature of 9.709587372 and 27.3461964 mm, respectively, for the IOL anterior and posterior surfaces was obtained through optimization by setting the solve type of the IOL posterior surface to be an element power of 0.022. During optimization, the IOL central thickness was constrained to be 0.8 mm.

(2) The IOL is aimed to provide a 1.5 D DOF, which corresponds to a continuous object distance ranging from 6 m to 0.66 m. To achieve this goal, a multi-configuration with different object distances was used for the following optimization, which is divided into two steps.

(3) Firstly, the object distances were set to be 6, 5, 4, 3, 2, and 1 m for each configuration. The weighting coefficient is slightly higher for the distance location in order to provide good far vision for human eyes. Because the pupil size changes with illuminations, two pupil sizes, 3 and 4.5 mm, are assigned to each configuration in order to make the IOL have robust performance for different pupil sizes. The 3 mm pupil diameter corresponds to photopic vision, whereas the 4.5 mm pupil diameter corresponds to mesopic vision. The IOL surface parameters including conic and aspheric coefficients α_{1i}, α_{2i} from the 4th to 10th order were set to be variable for optimization. A default merit function of root mean square (RMS) wavefront error was chosen for optimization. The IOL central and edge thickness was constrained to avoid the extreme geometries. The optimization was performed, respectively, for each zone until the MTF curves within the spatial frequency of 100 c/mm are greater than 0.1 for all configurations (6–1 m). The obtained parameters of the IOL surfaces were shown in Tables 2 and 3.

(4) Secondly, the IOL was optimized to further extend the DOF. The object locations were set roughly linearly, such as 1, 0.8, and 0.66 m for each configuration. The pupil diameter was set to be 3 mm for the best result that could be obtained under this pupil. A diffractive phase profile was added to the inner zone of the IOL anterior surface. The phase is described by

$$\phi_1 = M_1 \sum_{i=1}^{N} \beta_{1i} \rho_1^{2i}, \quad (\rho_1 = r/A_1), \quad (3)$$

Table 2. Parameters of the Inner Zone $(r \le A_1)$ of the IOL Surfaces

Parameter	Anterior Surface	Posterior Surface
Radius	9.709587372	−27.3461964
Conic	−28.4118202	−238.540327
α_{12}	-3.512×10^{-3}	-4.000×10^{-3}
α_{13}	9.2693×10^{-3}	8.7584×10^{-3}
α_{14}	3.3409×10^{-4}	3.0958×10^{-4}
α_{15}	-5.673×10^{-4}	-5.760×10^{-4}

Table 3. Parameters of the Outer Zone $(A_1 < r < A_2)$ of the IOL Surfaces

Parameter	Anterior Surface	Posterior Surface
Radius	-8.284×10^{32}	9.8627×10^{22}
Conic	6.4209×10^{28}	-7.770×10^{20}
α_{22}	−0.04177115	8.9829×10^{-3}
α_{23}	0.022429863	-3.600×10^{-3}
α_{24}	-3.545×10^{-3}	3.3071×10^{-4}
α_{25}	1.7654×10^{-4}	-9.637×10^{-6}

where β_{1i} is the diffractive phase coefficient on the $2i^{\text{th}}$ power of ρ_1, which is the normalized radial aperture coordinate, and M_1 is the diffraction order.

The diffractive phase coefficients from the 2nd to 10th order (β_{11}–β_{15}) of the inner zone ($r \le A_1$) of the IOL anterior surface were set to be variables for optimization. The diffraction order and the weighting coefficients for each configuration were set to 1 and 0.333, respectively. A default merit function of the RMS wavefront error was re-established to perform the optimization. The diffractive phase coefficients were optimized until the MTF curves for all configurations (1–0.66 m) are greater than 0.1 within the spatial frequency of 100 c/mm under a 3 mm pupil. The obtained diffractive phase coefficients of the inner zone ($r \le A_1$) of the IOL anterior surface were shown in Table 4. The diffractive profile of the IOL surface was obtained by running the Zemax programming language (ZPL) macro for the fabrication. The obtained radial coordinates of the diffractive rings are shown in Table 5. The step height of the ring is 1.123 μm.

Through the above optimization, a double-zone aspheric diffractive IOL with an optical zone of 6 mm, a central thickness of 0.8 mm, and an edge thickness of 0.149 mm was obtained. The cross-section profile of the effective optical zone of the IOL is shown in Fig. 1.

The IOL is designed to provide continuous clear vision for object distances ranging from 6 to 0.66 m. The theoretical optical performances of the aphakic model eye implanted with the designed IOL (hereafter, the pseudophakic model eye) were evaluated for different object distances. The 1.5 D DOF in the object space corresponds to a 0.380 mm DOF in the image space. This conversion makes it easier to compare the theoretical results with the experimental results of the manufactured IOL, which were evaluated in the image space due to the setting of the testing instrument.

Table 4. Diffractive Phase Coefficients of the Inner Zone ($r \le A_1$) of the IOL Anterior Surface

Inner Zone of the IOL Anterior Surface	Diffractive Phase Coefficients
β_{11}	−10.1338089
β_{12}	−92.4055217
β_{13}	235.7040698
β_{14}	−152.264561
β_{15}	−0.95913561

Table 5. Diffractive Rings of the Inner Zone ($r \le A_1$) of the IOL Anterior Surface

Cycles (m)	−1	−2	−3
Radius (mm)	0.963291	1.659442	1.739161

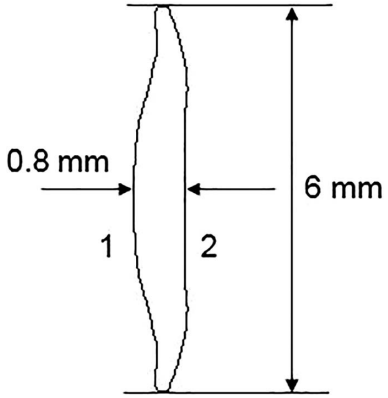

Fig. 1. Cross-section profile of the effective optical zone of the optimized IOL.

The MTF of the pseudophakic model eye was evaluated under a 3 mm pupil (photopic vision) at nine different object locations (6, 5, 4, 3, 2, 1.5, 1, 0.8, and 0.66 m) ranging from 6 to 0.66 m for 0° and 5° FOV. The results were shown in Fig. 2. The 5° FOV was taken into consideration in the analyses because the retinal fovea, where a large number of cones for the human eyes to resolve details are located[18], corresponds to a 5° FOV. The MTFs at 25 and 50 c/mm, as recommended by the International Organization for Standardization (ISO)[19,20], were used to analyze the imaging quality of the IOL in this study.

Figure 2(a) shows the MTF for 0° FOV. The MTF values are 0.40 to 0.90 at 25 c/mm and 0.35 to 0.80 at 50 c/mm, respectively, for all object locations, indicating good optical performance in photopic vision for object distances ranging from 6 to 0.66 m. The object distance of 0.8 m shows the best image quality for 0° FOV, as the MTF is higher than 0.90 at 25 c/mm and remains above 0.80 at 50 c/mm. Figure 2(b) shows the MTF for 5° FOV. Except for the object location of 0.8 m, only a slight decline of the MTF curves is observed in comparison with that for 0° FOV. The MTF values are 0.46 to 0.67 at 25 c/mm and 0.29 to 0.40 at 50 c/mm, respectively, for all object locations. The analyses above show that the pseudophakic model eye has quite good optical performance for the full ±5° FOV in photopic vision for object distance ranging from 6 to 0.66 m. Bellucci and Curatolo[21] also showed that the IOL performances were basically the same for 5° and 9° FOV in their study, exhibiting a consistency with this study. In other studies[13,22], the analyses of the EDOF IOLs usually focus on the performance of 0° FOV.

The visual acuity of the model eye implanted with the designed IOL and with a 22 D monofocal IOL in a 3 mm pupil was assessed using the simulated 20/20 Snellen E optotypes for a 1.5 D object vergence range. Figure 3 shows that the model eye with the designed IOL obtains clear images over the full 1.5 D range of the object vergence, whereas the model eye with the monofocal IOL can only obtain clear images for object vergence of 1 and 1.25 D.

Considering that the pupil diameter plays a critical role in the retinal image quality[23], the MTF at 50 c/mm of the

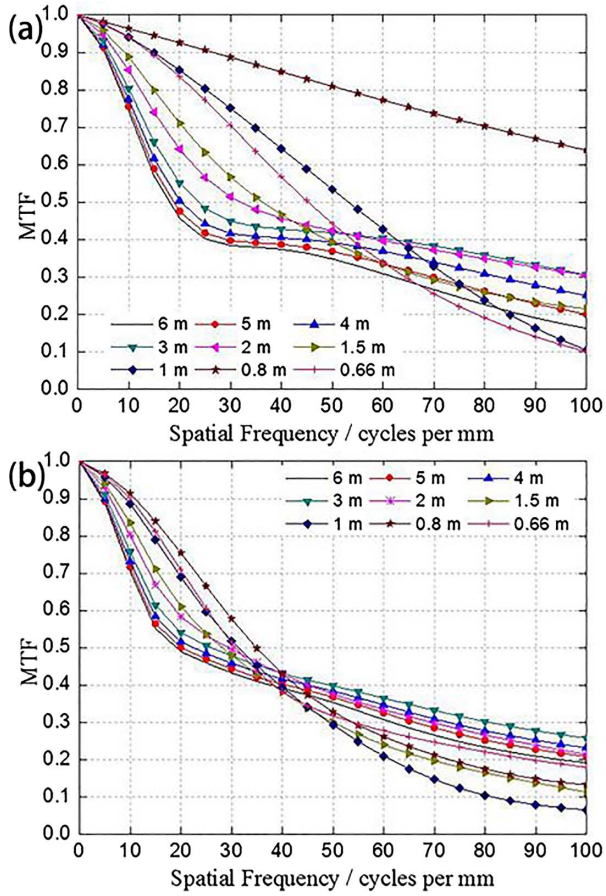

Fig. 2. MTF of the pseudophakic model eye under a 3 mm pupil at nine object locations for (a) 0° FOV and (b) 5° FOV. The MTF values are the average of tangential and sagittal directions.

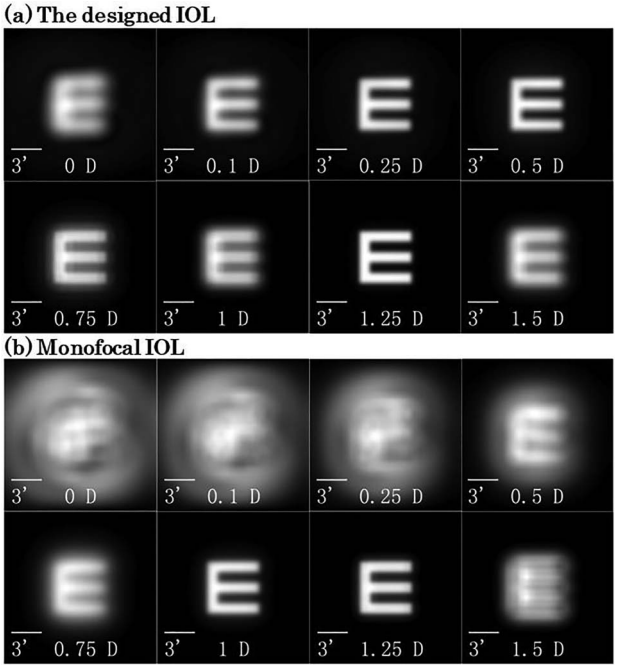

Fig. 3. Simulated 20/20 Snellen E optotypes of the model eye under a 3 mm pupil implanted with (a) the designed IOL and (b) a 22 D monofocal IOL for a 1.5 D object vergence.

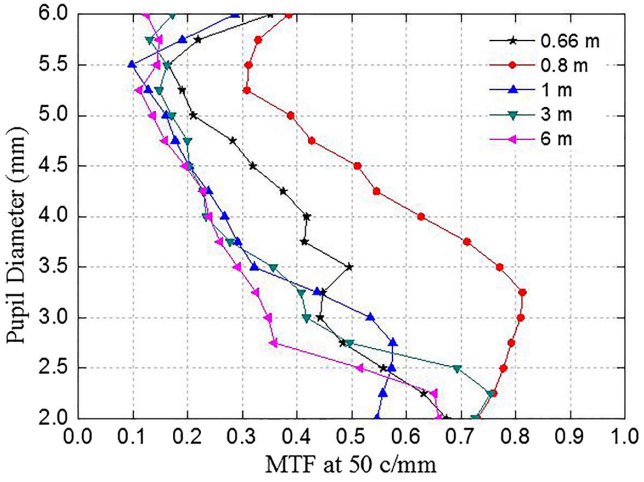

Fig. 4. MTF at 50 c/mm of the pseudophakic model eye for 0° FOV as a function of the pupil diameter at five object locations.

pseudophakic model eye as a function of the pupil diameter was evaluated for object locations ranging from 5 to 0.66 m. The results were shown in Fig. 4.

When the pupil diameter changes from 2 to 3.5 mm (corresponding to photopic vision), the MTF values are greater than 0.3 for all object locations and reach up to 0.81 at 0.8 m, which indicates that the imaging quality of the designed IOL is excellent in photopic vision. The MTF curves show a downward trend when the pupil diameter changes from 3.5 to 5.5 mm. However, all of the MTF values are still greater than 0.1 for pupil diameters changing from 2 to 6 mm. The scotopic vision requires relatively lower imaging resolution of the eye system. Therefore, it may be safe to state that the reduction of the MTF for scotopic vision is still acceptable. The analyses above show that the optical performance of the pseudophakic model eye remains acceptable when the pupil diameter changes from 2 to 6 mm.

Due to the fact that the human eyes work in white light environments, it is necessary to evaluate the optical performance of the designed IOL in such conditions. The polychromatic light with wavelengths of 470, 510, 555, 610, and 650 nm was selected, which represents the photopic visual spectrum. The weighting coefficients of the five wavelengths were set to 0.091, 0.503, 1, 0.503, and 0.107, respectively, based on the luminosity function curve of human eyes under the photopic condition. The MTF curves of the pseudophakic model eye in polychromatic light for 0° and 5° FOVs at nine object locations under a 3 mm pupil were shown in Fig. 5.

Figure 5(a) shows the MTF in polychromatic light for 0° FOV. The MTF values are 0.39 to 0.82 at 25 c/mm and 0.28 to 0.63 at 50 c/mm, respectively, for all object locations. Figure 5(b) shows the MTF in polychromatic light for 5° FOV. The MTF values are 0.43 to 0.62 at 25 c/mm and 0.25 to 0.34 at 50 c/mm, respectively, for all object locations. The MTF curves for polychromatic light show no obvious decline compared with that for monochromatic

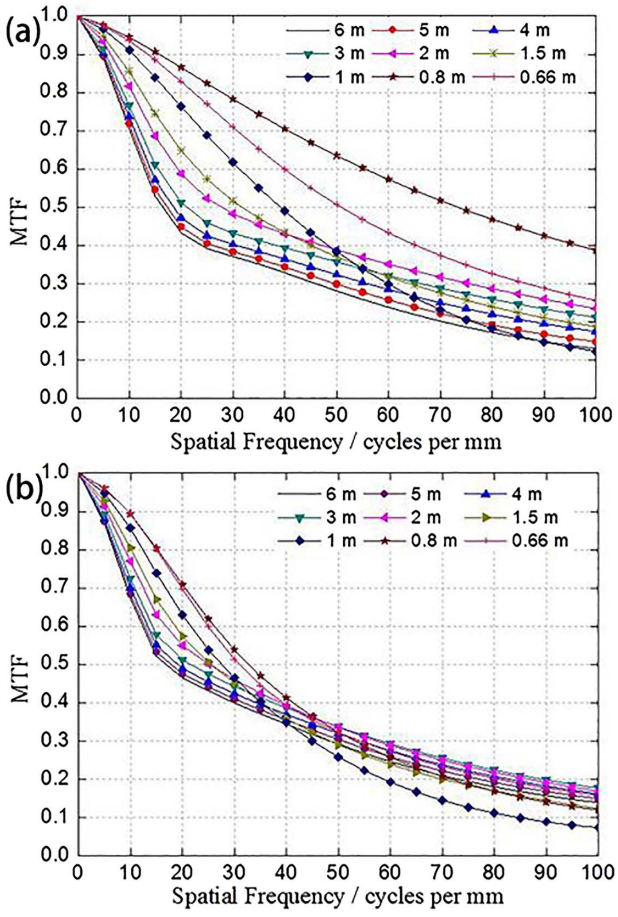

Fig. 5. MTF of the pseudophakic model eye in polychromatic light for (a) 0° FOV and (b) 5° FOV at nine object locations under the 3 mm pupil. The MTF values are the average of tangential and sagittal directions.

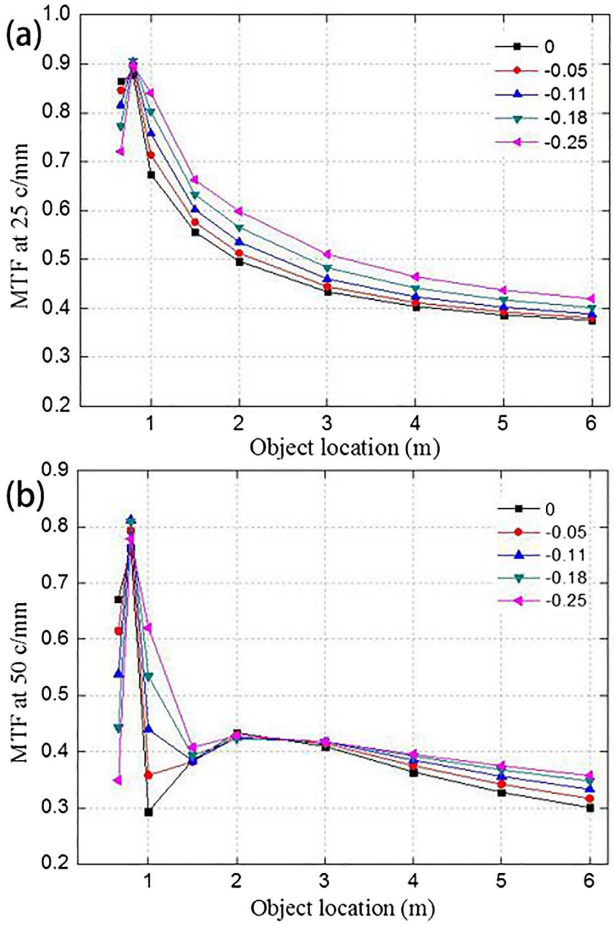

Fig. 6. MTF of five pseudophakic model eyes with different corneal aspherical coefficients at (a) 25 c/mm and (b) 50 c/mm as a function of the object distance for a 3 mm pupil and 0° FOV. The aspherical coefficient of the designed model eye is −0.18.

light in Fig. 2. This analysis shows that the image quality of the designed IOL is not noticeably affected by chromatic aberrations for the full ±5° FOV.

Because the corneal asphericity varies among individuals[24], the IOL performances were evaluated for different corneal aspherical coefficients. Five conic coefficients of the corneal anterior surface were selected for the pseudophakic model eyes. The MTFs at 25 and 50 c/mm of the pseudophakic model eyes under a 3 mm pupil as a function of the object distance were shown in Fig. 6. The MTF values at 25 and 50 c/mm are slightly affected by the variation of the corneal asphericities. The MTF values are 0.37 to 0.91 at 25 c/mm and 0.30 to 0.82 at 50 c/mm, respectively, for object distances ranging from 6 to 0.66 m. The result indicates that the optical performance of the designed IOL is relatively stable for different corneal asphericities.

The manufactured double-zone aspheric diffractive IOL is shown in Fig. 7. The measurement equipment of the Trioptics-OptiSpheric® IOL setup shown in Fig. 8 is used for the IOL testing. It belongs to the OptiSpheric® instrument line, which is the industry's standard for lens testing. The manufactured IOL is placed into the model eye of this

Fig. 7. Profile of the manufactured double-zone aspheric diffractive IOL.

setup. The image of the United States Air Force (USAF) test chart and the MTF can be examined in the focal plane of the model eye under 3 and 4.5 mm pupils. The microscope and CCD camera can be moved together continuously throughout the entire range of the DOF, and thus, several images of the USAF test chart and the MTF can be obtained during the moving process.

Figure 9 shows several images of the USAF test charts of the manufactured IOL in 3 and 4.5 mm pupils measured

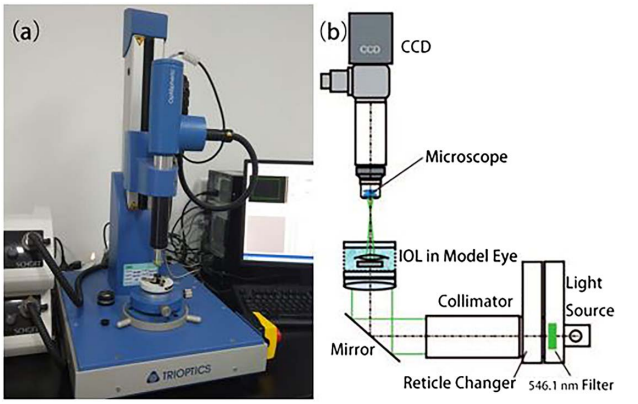

Fig. 8. Trioptics-OptiSpheric® IOL equipment for the IOL testing according to the EN/ISO 11979 standard: (a) setup, (b) schematic.

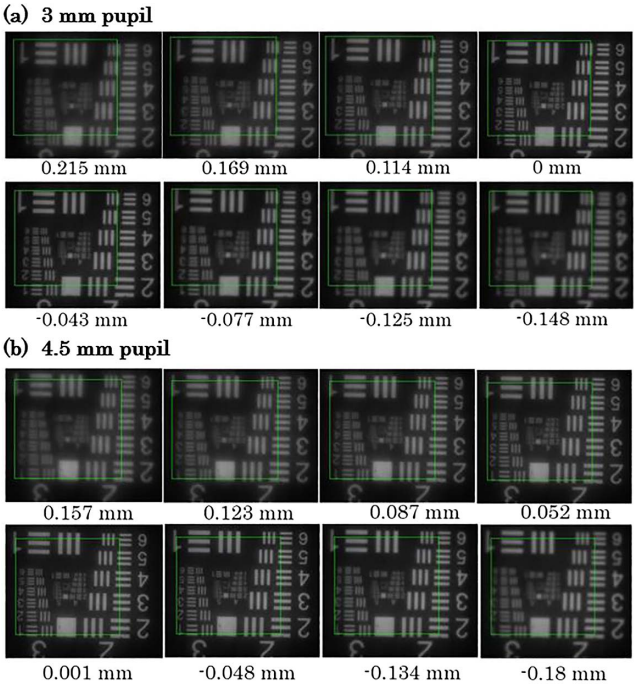

Fig. 9. USAF test charts at several focal positions of the manufactured IOL for (a) a 3 mm pupil and (b) a 4.5 mm pupil obtained from the Trioptics-OptiSpheric® IOL setup.

at eight focal planes, which are within the range of the designed DOF and randomly selected. The labeled values at the bottom of each image are the relative positions of the focal planes. The total relative distances of the measured USAF images are 0.363 mm under the 3 mm pupil and 0.337 mm under the 4.5 mm pupil, respectively, indicating that the experimental DOF is close to the theoretical DOF of 0.380 mm under the 3 mm pupil. The experimental testing results show that the designed IOL is able to extend the DOF.

Figure 10 shows six MTF curves of the manufactured IOL in 3 and 4.5 mm pupils separately measured at six randomly selected focal planes, which are in a continuous

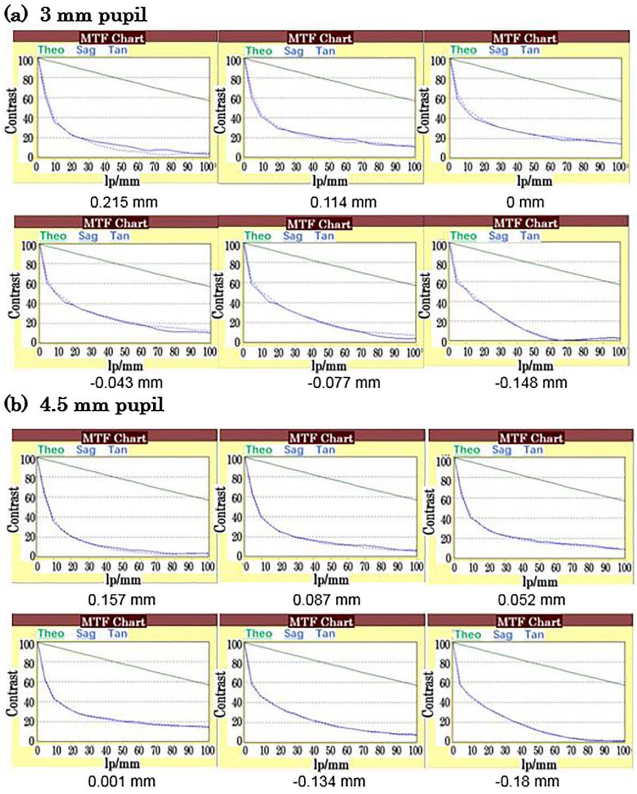

Fig. 10. MTF at several focal positions of the manufactured IOL for (a) a 3 mm pupil and (b) a 4.5 mm pupil obtained from the Trioptics-OptiSpheric® IOL setup. The higher line in each image is the diffraction-limited MTF. The labeled values at the bottom of each image are the relative positions of the focal planes.

range of the DOF. The MTF values at 25 c/mm are 0.20 to 0.35 under the 3 mm pupil and 0.15 to 0.30 under the 4.5 mm pupil for the full DOF, indicating declined image quality compared with the theoretical results. The results are similar to the study by Bellucci *et al.*[21]. However, the manufactured IOL shows the ability to extend the DOF despite the experimental testing results of the MTF being lower than the theoretical results.

The manufactured IOL surface profile error (the surface sag of the manufactured IOL minus the surface sag of the designed IOL) was measured with the instrument of Taylor Hobson Form Talysurf shown in Fig. 11.

Figure 12 shows the results of the profile error for the IOL anterior and posterior surfaces. The examined maximum aperture is 4.5 mm due to the limit of the instrument. The profile error varies with the aperture size of the IOL. The maximum difference of the IOL posterior surface is less than 40 μm for the whole 4.5 mm aperture. The maximum difference of the IOL anterior surface is less than 2 μm for the central 2 mm aperture, but up to 400 μm for the 4.5 mm aperture, which indicates that the central 2 mm area of the IOL basically meets the theoretical design, but the peripheral area of the IOL anterior surface is manufactured with larger errors.

The manufactured IOL was also examined with the Olympus IX71 microscope to observe its diffractive rings.

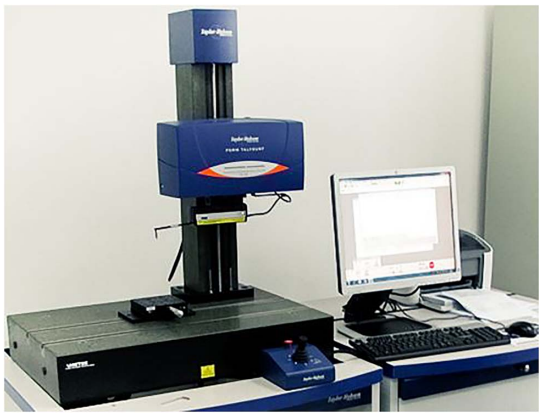

Fig. 11. Instrument of the Taylor Hobson® Form Talysurf.

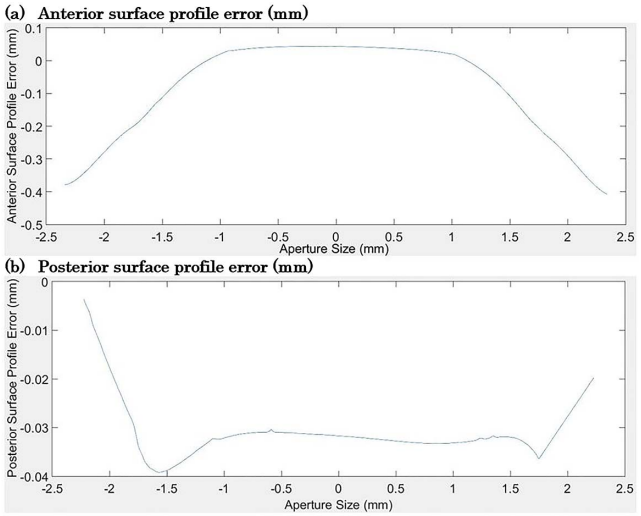

Fig. 12. IOL surface profile error obtained from the Taylor Hobson Form Talysurf (the surface sag of the manufactured IOL minus the surface sag of the designed IOL).

The result is shown in Fig. 13. The first diffractive ring is clearly observed, but the second and the third diffractive rings cannot be distinguished. The outermost ring is the edge of the IOL. The theoretical coordinates of the second and third diffractive rings are relatively close, which may increase the processing difficulty, resulting in failing to distinguish them in the manufactured IOL. In addition, the manufacture of the diffractive rings may also affect the profile error of the IOL anterior surface, thus resulting in the decline of the actual image quality.

In summary, a 22 D double-zone aspheric diffractive IOL was designed. The IOL implanted into the model eye achieves high-quality imaging for the full ±5° FOV for object distances ranging from 6 to 0.66 m in photopic vision. In addition, the presented theoretical analyses show that the optical performances of the designed IOL are relatively stable for pupil changes, polychromatic light, and different corneal asphericities, which has important practical significance for ophthalmic applications. Finally, the experimental DOF approaches the theoretical

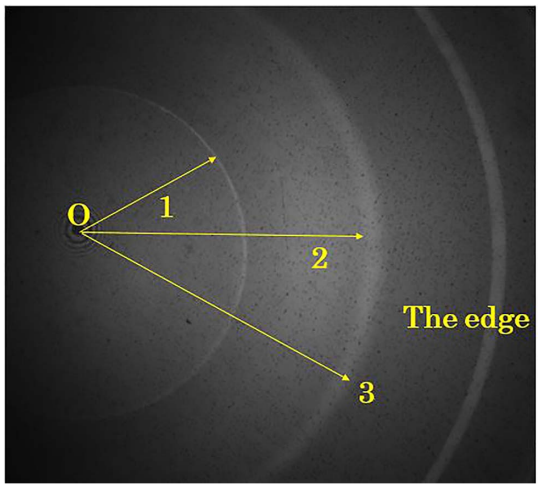

Fig. 13. Manufactured IOL profile obtained from the Olympus IX71 microscope (part of the IOL). The theoretical radial coordinates of the first, second, and third rings are $r_1 = 0.963291$ mm, $r_2 = 1.659442$ mm, and $r_3 = 1.739161$ mm, respectively.

value, showing that the designed IOL is able to provide an EDOF. Because the MTFs of the manufactured IOL are lower than the theoretical results, further improvements are needed to obtain an IOL that could be easily manufactured.

This work was supported by the National Natural Science Foundation of China (No. 11474172).

References

1. K. Petelczyc, S. Bará, A. C. Lopez, Z. Jaroszewicz, K. Kakarenko, A. Kolodziejczyk, and M. Sypek, Opt. Express **19**, 25602 (2011).
2. S. R. Flaxman, R. R. A. Bourne, S. Resnikoff, P. Ackland, T. Braithwaite, M. V. Cicinelli, A. Das, J. B. Jonas, J. Keeffe, J. H. Kempen, J. Leasher, H. Limburg, K. Naidoo, K. Pesudovs, A. Silvester, G. A. Stevens, N. Tahhan, T. Y. Wong, and H. R. Taylor, Lancet Glob Health. **5**, e1221 (2017).
3. J. Tang and Y. Deng, Pract. J. Clin. Med. **11**, 7 (2014).
4. M. Kong, Z. Gao, L. Chen, and X. Li, Chin. Opt. Lett. **6**, 377 (2008).
5. M. Kim, J. H. Kim, T. H. Lim, and B. J. Cho, Korean J. Ophthalmol. **32**, 77 (2018).
6. J. A. Davison and M. J. Simpson, J. Cataract Refract. Surg. **32**, 849 (2006).
7. R. Montés-Micó and J. L. Alió, J. Cataract Refract. Surg. **29**, 703 (2003).
8. M. Packer, I. H. Fine, and R. S. Hoffman, J. Cataract Refract. Surg. **28**, 421 (2002).
9. Y. Liu, X. Wang, and Z. Wang, "Movable aspheric intraocular lens with extended visual range," Chinese Patent ZL201510292026.2 (2015).
10. J. S. Cumming, S. G. Slade, and A. Chayet, and the AT-45 Study Group, Ophthalmology **108**, 2005 (2001).
11. A. Langenbucher, S. Huber, N. X. Nguyen, B. Seitz, G. C. Gusek-Schneider, and M. Küchle, J. Cataract Refract. Surg. **29**, 677 (2003).
12. J. S. Pepose, J. Burke, and M. A. Qazi, Curr. Opin. Ophthalmol. **28**, 3 (2017).
13. H. A. Weeber, S. T. Meijer, and P. A. Piers, J. Cataract Refract. Surg. **41**, 2746 (2015).
14. R. Fan and Y. Liu, Laser Optoelectron. Progress **52**, 051701 (2015).

15. A. Mira-Agudelo, W. Torres-Sepulveda, J. F. Barrera, R. Henao, N. Blocki, K. Petelczyc, and A. Kolodziejczyk, Invest. Ophth. Vis. Sci. **57**, 6870 (2016).
16. D. Fernández, S. Barbero, C. Dorronsoro, and S. Marcos, Opt. Lett. **38**, 5303 (2013).
17. L. Jiang, Y. Liu, X. Wang, and Z. Wang, Proc. SPIE. **10021**, 1002115 (2016).
18. S. Zheng, Z. Wang, Y. Liu, and R. Li, Appl. Opt. **51**, 6926 (2012).
19. International Organization for Standardization, ISO 11979–9 (2006).
20. International Organization for Standardization, ISO 11979–2 (2014).
21. R. Bellucci and M. C. Curatolo, J. Refract. Surg. **33**, 389 (2017).
22. J. J. Esteve-Taboada, A. Domínguez-Vicent, A. J. Del Águila-Carrasco, T. Ferrer-Blasco, and R. Montés-Micó, J. Refract. Surg. **31**, 666 (2015).
23. W. N. Charman, Ophthalmic Physiol. Opt. **37**, 1 (2017).
24. M. Kong, Z. Gao, X. Li, S. Ding, X. Qu, and M. Yu, Opt. Express **17**, 13283 (2009).